



**Acoustics'08  
Paris**  
June 29-July 4, 2008

[www.acoustics08-paris.org](http://www.acoustics08-paris.org)

## Investigation of effect of trabecular microstructure on ultrasound propagation through cancellous bone using finite-difference time-domain simulations

Atsushi Hosokawa

Akashi National College of Technology, 679-3 Nishioka, Uozumi, 674-8501 Akashi, Japan  
hosokawa@akashi.ac.jp

The effect of the trabecular microstructure on the propagation of ultrasound waves through cancellous bone was numerically investigated by finite-difference time-domain (FDTD) simulation. In a three-dimensional (3-D) numerical model reconstructed from a 3-D micro-computed tomography ( $\mu$ CT) image of bovine cancellous bone, the trabecular elements were eroded to increase the porosity using an image processing technique. Three erosion procedures were given to realize different changes in the trabecular microstructure with increasing the porosity. The FDTD simulation of the ultrasound pulse waves propagating through the eroded cancellous bone model was performed in two cases of the propagations parallel and perpendicular to the major trabecular orientation. The propagation properties of the wave amplitude and speed in each propagation direction were simulated as functions of the porosity, and their variability depending on the trabecular microstructure was revealed. The effects of the microstructures in the major and minor trabecular directions were investigated from the correlation coefficients of the propagation properties with the mean intercept lengths (MILs) of the trabecular elements in the two directions.

## 1 Introduction

Ultrasound techniques have played a significant role for diagnostic assessment of osteoporosis. Among typical techniques, the speed of sound (SOS) and broadband ultrasound attenuation (BUA) are measured at the site including cancellous bone with a trabecular structure oriented perpendicular to the ultrasound propagation [1,2]. A novel technique considering the propagation of the fast and slow waves, which can be clearly observed in the direction of the major trabecular orientation [3-5], is also under development [6,7]. However, the residual variability of the ultrasound parameters has been observed in both cases [6-8]. This appears to be because the trabecular structure can affect the ultrasound propagation through cancellous bone. It was experimentally demonstrated that the major trabecular orientation could largely be related to the propagation phenomenon in the bone [3-5], whereas it is not sufficiently investigated how the trabecular microstructure can affect the propagation. However, the detailed investigation of this effect using experimental approaches is difficult because of the variable trabecular microstructure.

In this study, the effects of the trabecular microstructure on the ultrasound pulse wave propagations through bovine cancellous bone, in two cases of the propagation directions parallel and perpendicular to the major trabecular orientation, were numerically investigated by FDTD simulation with the cancellous bone model reconstructed from a 3-D  $\mu$ CT image. In the cancellous bone model, distinct changes in the trabecular microstructure with increasing the porosity were realized by giving three erosion procedures. To examine the respective effects of the microstructures in the major and minor trabecular directions, the attenuation (amplitude) and propagation speed were derived as functions of the porosity plus the MILs of the trabecular elements in the two directions.

## 2 Numerical implementation

### 2.1 Numerical cancellous bone model

A numerical cancellous bone model of  $6.45 \times 6.45 \times 6.45$  mm<sup>3</sup> were reconstructed from the 3-D  $\mu$ CT image of a bovine femoral cancellous bone specimen with porosity of

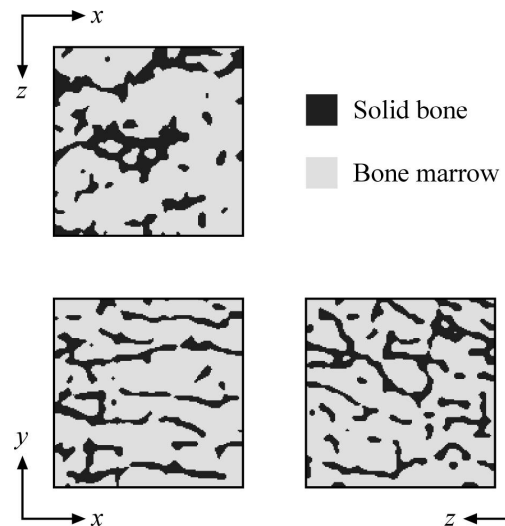


Fig.1 Trabecular structure of 3-D  $\mu$ CT cancellous bone model with porosity of 0.76 (prior to erosion).

0.76 (76 %). The voxel size of the cancellous bone model was  $64.5 \mu\text{m}$ . The grayscale values in all spatial points were downgraded to binary ones in order to clearly separate between two parts of the solid bone (trabecula) and pore space, and it was assumed that all points of the pore space were perfectly saturated with bone marrow. The two-dimensional (2-D) trabecular structures on three orthogonal planes of the cancellous bone model are illustrated in Fig.1. The  $x$ -,  $y$ -, and  $z$ -directions respectively correspond to the longitudinal, transverse, and sagittal ones in the general anatomic coordinates. As shown in Fig.1, a strong (or major) orientation of the trabecular elements in the  $x$ -direction and a weak orientation in the  $z$ -direction can be observed, and therefore the  $y$ -direction is perpendicular to the trabecular orientation.

Using an image processing technique, the trabecular elements in the cancellous bone model were eroded to increase the porosity [9,10]. Three erosion procedures were given to realize distinct changes in the trabecular microstructure with increasing the porosity. In the erosion procedure A, the erosions applied to the points of the solid bone, that is the transformations of the surface points of the trabecular elements from the solid bone to bone marrow, were randomly distributed in every direction. In the erosion procedure B, the distribution of the erosions was weighed in the  $x$ -direction (namely the major trabecular direction), and in the erosion procedure C, the distribution was weighed in the  $y$ -direction (the minor trabecular direction). To quantitatively estimate the trabecular change, the

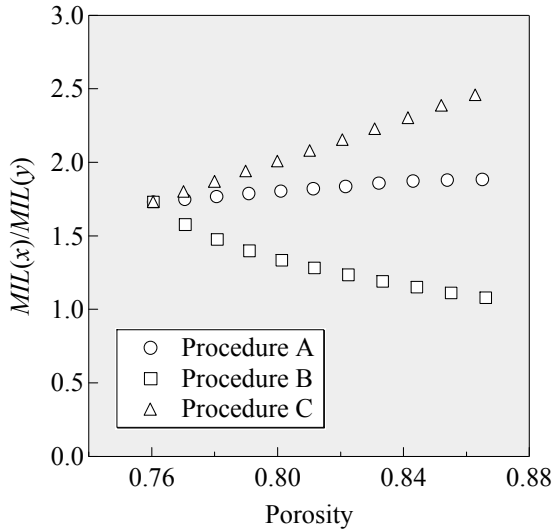


Fig.2 Variations in anisotropic parameter of trabecular structure with increasing porosity in three erosion procedures.

anisotropic parameter of  $MIL(x)/MIL(y)$  was introduced, where  $MIL(\xi)$  is the MIL of the trabecular elements in the  $\xi$ -direction ( $\xi = x, y$ ). As the trabecular anisotropy becomes stronger, the value of  $MIL(x)/MIL(y)$  becomes larger. The variation in this parameter value of the cancellous bone model with increasing the porosity in each erosion procedure is shown in Fig. 2. The circular, square, and triangular marks respectively show the data in the erosion procedures A, B, and C, which is common notation in this paper. In Fig. 2, the parameter value in the erosion procedure A is almost constant, whereas the values in the procedures B and C respectively decrease and increase with the porosity. Thus, the trabecular microstructure could be changed using the distinct methods for eroding the trabecular elements.

## 2.2 FDTD simulation model

For an isotropic viscoelastic medium, the particle velocity components  $\dot{u}_\xi$  and stress components  $\tau_{\xi\xi}$ ,  $\tau_{\xi\psi}$  are related by the following first-order partial differential equations:

$$\rho \frac{\partial \dot{u}_\xi}{\partial t} = \frac{\partial \tau_{\xi\xi}}{\partial \xi} + \frac{\partial \tau_{\xi\psi}}{\partial \psi} + \frac{\partial \tau_{\xi\zeta}}{\partial \zeta}, \quad (1)$$

$$\frac{\partial \tau_{\xi\xi}}{\partial t} + \gamma_{\xi\xi} \tau_{\xi\xi} = (\lambda + 2\mu) \frac{\partial \dot{u}_\xi}{\partial \xi} + \lambda \frac{\partial \dot{u}_\psi}{\partial \psi} + \lambda \frac{\partial \dot{u}_\zeta}{\partial \zeta}, \quad (2)$$

$$\frac{\partial \tau_{\xi\psi}}{\partial t} + \gamma_{\xi\psi} \tau_{\xi\psi} = \mu \left( \frac{\partial \dot{u}_\xi}{\partial \psi} + \frac{\partial \dot{u}_\psi}{\partial \xi} \right), \quad (3)$$

where  $\xi, \psi, \zeta = x, y, z$ . In Eqs.(1)-(3),  $\rho$  is the medium density,  $\lambda$  and  $\mu$  are the Lamé coefficients, and  $\gamma_{\xi\xi}$  and  $\gamma_{\xi\psi}$  are the resistance coefficients related to the attenuation coefficients [11]. In the viscoelastic FDTD method, the partial differentiations in these equations are approximated using a central differencing scheme with staggered grids. Using the discrete equations, the particle velocity and stress values are alternately calculated in both spatial and temporal domains [12].

The whole region of the FDTD simulation model for

Parameter	Solid bone	Bone marrow
First Lamé coefficient $\lambda$ (GPa)	14.8	2.0
Second Lamé coefficient $\mu$ (GPa)	8.3	0
Density $\rho$ (kg/m <sup>3</sup> )	1960	930
Normal resistance coefficient $\gamma_{\xi\xi}$	$8 \times 10^4$	$3 \times 10^3$
Shear resistance coefficient $\gamma_{\xi\psi}$	$8 \times 10^5$	0

Table 1 Physical parameters of bovine cancellous bone used in FDTD simulations [13]

ultrasound propagation through cancellous bone was  $11.45 \times 6.45 \times 6.45 \text{ mm}^3$ . The FDTD simulations were performed for two propagations in the  $x$ - and  $y$ -directions corresponding to the major and minor trabecular directions in the cancellous bone model. Then, the transmitting and receiving circular surfaces with 6.45 mm diameter were placed on the  $y$ - $z$  planes at  $x = 0$  and 11.45 mm or on  $z$ - $x$  planes at  $y = 0$  and 11.45 mm. The water regions of  $2.5 \times 6.45 \times 6.45 \text{ mm}^3$  were set between the transmitting surface and the cancellous bone model and between the cancellous bone model and the receiving surface. As for the excitation condition, a pulsed particle displacement in the propagation direction was given at the corresponding points on the transmitting surface. The time function was a single sinusoid at 0.75 MHz multiplied by a Hamming window. The output was calculated as the summation of the pressures at all receiving points.

The viscoelastic FDTD method described above was used for the calculation in the region of the cancellous bone model, and the acoustic FDTD method for acoustic wave propagation was used in the water region. The spatial interval was  $64.5 \mu\text{m}$  in order to adapt the voxel size of the cancellous bone model, and the time interval was 5.16 ns in order to satisfy the stability condition in the FDTD method. Table I [13] lists the physical parameter values used in the FDTD simulations. A pulse waveform propagating through the cancellous bone model at each eroded step was calculated, and the propagation properties of attenuation (amplitude) and propagation speed were derived. The peak-to-peak amplitude was normalized to that of the simulated waveform propagating in water only without the cancellous bone model, and the wave speed was obtained from the difference in the propagation time between the simulated waves with and without the cancellous bone model.

## 3 Simulated results

### 3.1 Propagation properties in the major trabecular direction

In all simulated waveforms using the eroded cancellous bone model for the propagation in the major trabecular direction ( $x$ -direction), both the fast and slow waves could be observed, similarly to the previous experimental results

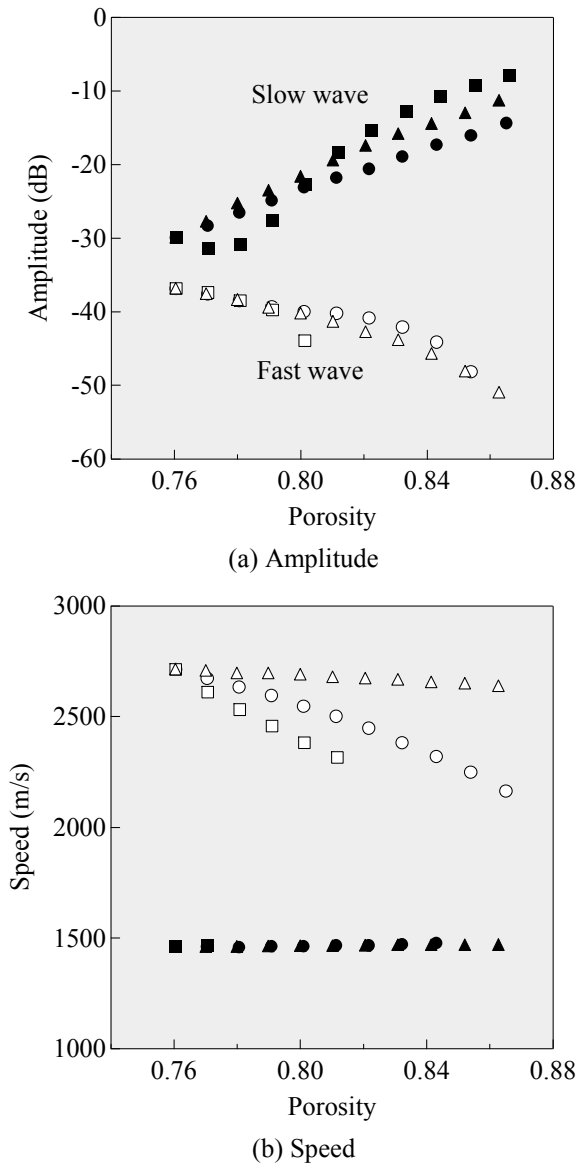


Fig.3 Propagation properties of the fast and slow waves through the cancellous bone model in the major trabecular direction, as a function of porosity varied by erosion procedures A (circles), B (squares), and C (triangles).

[3-5]. The derived propagation properties of the fast and slow waves are shown in Fig.3, as a function of the porosity varied by three erosion procedures A, B, and C (several values at high porosities could not be derived because the fast and slow waveforms were not distinctly separated). Figures 3(a) and (b) respectively shows the wave amplitudes and speeds. In Fig.3(a), the fast and slow wave amplitudes respectively decrease and increase with increasing the porosity in all erosion procedures. Moreover, the fast wave amplitude is scarcely varied with the erosion procedure, that is the change in the trabecular microstructure (the amplitude value at porosity of about 0.8 in the erosion procedure B probably contains a large error due to the overlap of the fast and slow waveforms), whereas the slow wave amplitude is largely affected by the trabecular microstructure although its relationship is not clear in Fig.3(a). In Fig.3(b), the fast wave speed linearly decreases with the porosity, and its slope is largest in the erosion procedure B and smallest in the procedure C. Thus, the variation in the fast wave speed with the porosity depends the erosion procedure or the trabecular

Parameter	Amplitude		Speed	
	Fast wave	Slow wave	Fast wave	Slow wave
Porosity	-0.89	0.95	-0.54	0.61
$MIL(x)$	0.48	-0.63	0.92	-0.81
$MIL(y)$	0.82	-0.83	0.41	-0.52
$MIL(x)/MIL(y)$	-0.41	-0.04	0.35	0.06

Table II Correlation coefficients of propagation properties of the fast and slow waves through the eroded cancellous bone model in the major trabecular direction with four structural parameters

microstructure. On the other hand, the slow wave speed is almost constant without relation to both the porosity and the trabecular microstructure.

It was shown that the propagation properties of both the fast and slow waves largely depended on (or varied with) the porosity, except for the slow wave speed. However, it was not clear how the propagation properties are related to the trabecular microstructure, although the distinct changes in the trabecular microstructure with increasing the porosity were realized by three erosion procedures, as shown in the variations in the anisotropic parameter  $MIL(x)/MIL(y)$  (Fig.2). This appears to be because the microstructures in both the major and minor trabecular directions ( $x$ - and  $y$ -directions) changed with the erosion. Specifically, it can be considered that the propagation properties are affected by the trabecular microstructure in either direction rather than the entire anisotropic structure. Therefore, the relationships of the propagation properties to the microstructure in each trabecular direction must be clarified. Then, the correlation coefficients of the propagation properties with four parameters of the porosity, the MILs of the trabecular elements in the major and minor trabecular directions [ $MIL(x)$ ,  $MIL(y)$ ], and the anisotropic parameter [ $MIL(x)/MIL(y)$ ], were calculated using all data in three erosion procedures.

Table II lists the calculated correlation coefficients of the amplitudes and speeds of the fast and slow waves in the major trabecular direction. In Table II, the correlation coefficients of the fast and slow wave amplitudes with the porosity are -0.91 and 0.96, respectively, and therefore both amplitudes are strongly correlated with the porosity. In addition, the strong correlations with  $MIL(y)$  are also found (the absolute correlation coefficients are above 0.8). Accordingly, the fast and slow wave amplitudes primary depends on the porosity, and the porosity dependences can be affected by the microstructure in the minor trabecular direction.

It can be considered that the fast wave speed primary depends on the microstructures in the major trabecular direction because the correlation coefficient with  $MIL(x)$  is about 0.9. Although the correlation coefficient with the porosity, which was calculated using all data in three erosion procedures, is very low (about -0.45), the fast wave speed in Fig.3(b) linearly decreases with the porosity in any erosion procedure. It therefore appears that the strong correlation with the porosity is observed when the trabecular microstructure regularly changes with the porosity. On the other hand, the slow wave speed is

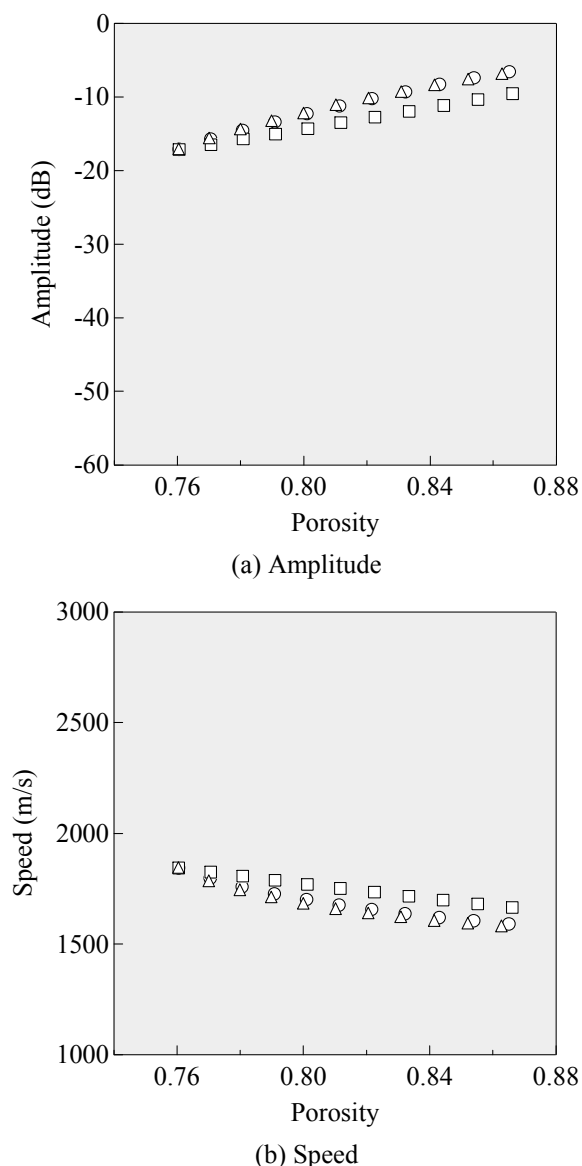


Fig.4 Propagation properties of an ultrasound wave through the cancellous bone model in the minor trabecular direction, as a function of porosity varied by erosion procedures A (circles), B (squares), and C (triangles).

moderately correlated with all parameters except for  $MIL(x)/MIL(y)$  (the absolute correlation coefficient: 0.67-0.79). Regrettably, it is impossible to interpret which parameter is most strongly related to the slow wave speed. This is because exactly measuring the propagation time of the slow wave is difficult due to the overlap of the fast waveform with the slow one.

### 3.2 Propagation properties in the minor trabecular direction

For the propagation in the minor trabecular direction ( $y$ -direction), a single wave could be observed in all simulated waveforms. The amplitude and speed of this wave as a function of the porosity are shown in Figs.4(a) and (b), respectively. In Fig.4(a), the amplitudes in all erosion procedures increase with the porosity, and its slope in the procedure B is smaller than those in the procedures A and C (the amplitudes in the procedures A and C are almost the same). In Fig.4(b), all speeds decrease with the porosity,

Parameter	Amplitude	Speed
Porosity	0.94	-0.88
$MIL(x)$	-0.31	0.19
$MIL(y)$	-0.99	0.99
$MIL(x)/MIL(y)$	0.37	-0.48

Table III Correlation coefficients of propagation properties of an ultrasound wave through the eroded cancellous bone model in the minor trabecular direction with four structural parameters

and its slope in the erosion procedure B is smallest, similarly to the amplitude. Thus, both propagation properties are affected by the trabecular microstructure due to the erosion. However, these variations are much smaller than those of the slow wave amplitude and fast wave speed in the major trabecular direction.

Table III lists the correlation coefficients calculated for the propagation properties in the minor trabecular direction. In Table III, both the amplitude and speed are strongly correlated with the porosity (the correlation coefficients are 0.97 and -0.93, respectively). The strong correlations with  $MIL(y)$  are also found (correlation coefficient: -0.99 and 0.99, respectively). The stronger correlations with  $MIL(y)$  than with the porosity mean that the propagation properties in the minor trabecular direction depend on the area porosity perpendicular to the major trabecular orientation rather than the total porosity, i.e., the ultrasound propagation in the minor trabecular direction can be little affected by the trabecular change perpendicular to the propagation direction.

All absolute correlation coefficients of the propagation properties in both the major and minor trabecular directions with  $MIL(x)/MIL(y)$  are low (0.5 at most). It can therefore be concluded that the propagation properties in both directions are little related to the trabecular anisotropy itself, as investigated in Sec.3.1.

## 4 Discussions

The widely used ultrasound parameters of BUA and SOS for diagnosis of osteoporosis are derived by measuring the transmitted ultrasound wave in the direction perpendicular to the major trabecular orientation. In this study, it was shown that the propagation properties of both the amplitude and speed in the minor trabecular direction, although the derived amplitude is different from BUA, depended on the porosity and the trabecular length in the propagation direction. Therefore, it can be considered that the bone volume (or area) fraction can be directly evaluated from BUA and SOS, and that their variability induced by the other structural factors is little. In conclusion, the diagnosis using BUA and SOS may be relatively stable in the evaluation of the bone density. However, evaluating the microstructure in the major trabecular direction, which is more closely related to the bone strength in the direction of stress applied by external loads such as weight, may be difficult.

At present, a novel diagnostic technique using the propagation properties of the fast and slow waves in the

major trabecular direction is proposed [6,7]. This study showed that these wave properties were affected by not only the porosity but also the trabecular microstructure in both the major and minor trabecular directions. Accordingly, it can be expected that the residual variability in the fast and slow wave parameters due to the effect of the trabecular microstructure is much larger than that in BUA and SOS. Conversely, there is possibility that the detailed trabecular microstructure can be evaluated by utilizing various relationships between the two wave properties and the structural parameters.

Although the propagation properties only in the parallel and perpendicular directions were investigated in this study, more complicated properties is speculated in the case of an oblique propagation. Accordingly, it can be considered that, in both diagnostic techniques utilizing the parallel and perpendicular propagation, large variability in the ultrasound parameters can be caused by the change in the propagation angle.

## 5 Conclusions

In this study, numerical analysis of the ultrasound propagation properties in cancellous bone with an oriented trabecular structure was performed by the FDTD simulation with the 3-D  $\mu$ CT cancellous bone model. By variously changing the trabecular microstructure with increasing the porosity using three erosion procedures, the propagation properties of the amplitudes and propagation speeds in two orthogonal directions were derived as functions of the porosity and the MILs of the trabecular elements. In the case of the fast and slow wave propagations parallel to the major trabecular orientation, both wave amplitudes were affected by the microstructure in the minor trabecular direction, whereas the fast wave speed was largely affected by the major trabecular elements, although these properties primary depended on the porosity. In the case of the propagation in the minor trabecular direction, on the other hand, both the amplitude and speed strongly depended on only two parameters of the porosity and the trabecular length in the propagation direction, which showed little effect of the microstructure in the major trabecular direction. To reduce the residual variability in the ultrasound parameters used in the diagnosis of osteoporosis, consequently, the structural effect concerning each propagation property must be sufficiently considered.

## Acknowledgments

This study was supported by a Grant-in-Aid for Young Scientists (B) (Grant No. 19700393) from the Ministry of Education, Culture, Sports, Science and Technology (MEXT) of Japan, and in part, by a Grant-in-Aid for Scientific Research (B) (Grant No. 19360189) from the Japan Society for the Promotion of Science (JSPS), by the Academic Frontier Research Project on "New Frontier of Biomedical Engineering Research" of Doshisha University and MEXT, and by JSPS and CNRS under the Japan-France Research Cooperative Program.

## References

- [1] C. M. Langton, S. B. Palmer, R. W. Porter, "The measurement of broadband ultrasonic attenuation in cancellous bone", *Eng. Med.* 13, 89-91 (1984)
- [2] P. J. Rossman, J. A. Zagzebski, C. Mesina, J. Sorenson, R. B. Mazess, "Comparison of speed of sound and ultrasound attenuation in the os calcis to bone density of the radius, femur, and lumbar spine", *Clin. Phys. Physiol. Meas.* 10, 353-360 (1989)
- [3] A. Hosokawa, T. Otani, "Ultrasonic wave propagation in bovine cancellous bone", *J. Acoust. Soc. Am.* 101, 558-562 (1997)
- [4] A. Hosokawa, T. Otani, T. Suzaki, Y. Kubo, S. Takai, "Influence of trabecular structure on ultrasonic wave propagation in bovine cancellous bone", *Jpn. J. Appl. Phys.* 36, 3233-3237 (1997)
- [5] A. Hosokawa, T. Otani, "Acoustic anisotropy in bovine cancellous bone", *J. Acoust. Soc. Am.* 103, 2718-2722 (1998)
- [6] T. Otani, "Quantitative estimation of bone density and bone quality using acoustic parameters of cancellous bone for fast and slow waves", *Jpn. J. Appl. Phys.* 44, 4578-4582 (2005)
- [7] I. Mano, K. Horii, S. Takai, T. Suzaki, H. Nagaoka, T. Otani, "Development of novel ultrasonic bone densitometry using acoustic parameters of cancellous bone for fast and slow waves", *Jpn. J. Appl. Phys.* 45, 4700-4702 (2006)
- [8] F. Jenson, F. Padilla, V. Bousson, C. Bergot, J.-D. Laredo, P. Laugier, "In vitro ultrasonic characterization of human cancellous femoral bone using transmission and backscatter measurements: Relationship to bone mineral density", *J. Acoust. Soc. Am.* 119, 654-663 (2006)
- [9] G. Luo, J. J. Kaufman, A. Chiabrera, B. Bianco, J. H. Kinney, D. Haupt, J. T. Ryaby, R. S. Siffert, "Computational methods for ultrasonic bone assessment", *Ultrasound Med. Biol.* 25, 823-830 (1999)
- [10] G. Haiat, F. Padilla, F. Peyrin, P. Laugier, "Variation of ultrasonic parameters with microstructure and material properties of trabecular bone: A 3-D model simulation", *J. Bone Miner. Res.* 22, 665-674 (2007)
- [11] N. Endoh, T. Tsuchiya, Y. Saito, "Development of ultrasonic propagation analysis method for estimation of inner state of bone phantom", *Jpn. J. Appl. Phys.* 44, 4598-4599 (2005)
- [12] J. Virieux, "P-SV wave propagation in heterogeneous media: Velocity-stress finite-difference method", *Geophysics* 51, 889-901 (1986)
- [13] A. Hosokawa, "Development of a numerical cancellous bone model for finite-difference time-domain simulations of ultrasound propagation", *IEEE Trans. Ultrason. Ferroelect. Freq. Contr.*, to be published